Int J Adv Manuf Technol (2018) 95:299–310
https://doi.org/10.1007/s00170-017-1197-x

ORIGINAL ARTICLE

Hot cracking behaviour of an autogenously laser welded Al-Cu-Li alloy

J. Enz[1] · C. Carrarin[1] · S. Riekehr[1] · V. Ventzke[1] · N. Kashaev[1]

Received: 6 July 2017 / Accepted: 6 October 2017 / Published online: 18 October 2017

Abstract AA2198 is a relatively new light-weight and high-performance Al-Cu-Li alloy considered for aviation and space applications. However, Al-Cu-Li alloys generally exhibit severe weldability problems for all fusion-welding techniques, such as laser-beam welding. In particular, porosity formation and hot cracking are observed for the laser-beam welding of these alloys. A common remedy for hot cracking is the use of an appropriate filler wire with a high Si content. In the present study, three different approaches for improving the hot cracking susceptibility of AA2198 laser beam welded without any filler material are presented. For this purpose, pre-heating of the weld samples to elevated temperatures, pre-loading of the weld samples perpendicular to the welding direction, or an optimization of the laser-beam welding parameters were conducted. The autogenously welded samples were assessed with regard to the resulting total crack length and their mechanical properties. It was demonstrated that all of the presented approaches led to a reduction of hot cracking. However, the largest effect was observed for the use of low levels of laser power and welding velocity. The mechanical properties of the optimised autogenously welded samples are only marginally inferior as for the samples laser welded with the Al-Si filler wire AA4047.

Keywords Al-Li alloy · Laser welding · Autogenous welding · Hot cracking · Mechanical properties

✉ J. Enz
josephin.enz@hzg.de

[1] Helmholtz-Zentrum Geesthacht, Institute of Materials Research, Materials Mechanics, Max-Planck-Straße 1, 21502 Geesthacht, Germany

1 Introduction

Al-Cu-Li alloys were developed for light-weight and high-performance applications in the aviation and space industry. In comparison to conventional Al-Cu alloys, Li-bearing Al-Cu alloys, such as AA2198, feature considerable higher specific strength and specific stiffness (according to Kostrivas and Lippold [1]). Moreover, the higher specific modulus leads to a reduction of the fatigue crack propagation, as explicated by Srivatsan [2]. The properties of these alloys are also adjusted by certain heat treatments, which is generally a sequence of solution heat treatment, cold working either followed by natural ageing (T3X) or by artificial ageing (T8X). According to Giummarra et al. [3], the strengthening is provided by the stable T_1 (Al_2CuLi), the metastable Θ'-type (Al_2Cu) and δ' (Al_3Li) precipitates. Whereas the stable T_2 (Al_6CuLi_3) precipitates increase the toughness. However, these promising alloys also exhibit severe weldability problems for all fusion-welding techniques. Even for laser-beam welding, generally resulting in a considerable lower heat input as conventional fusion-welding techniques, such as gas metal arc and gas tungsten arc welding, these weldability problems are observed [2]. Besides porosity formation, hot cracking is one of the major problems of welded Al-Cu alloys. In general, Li-bearing Al-Cu alloys can exhibit a high hot cracking susceptibility (HCS), as described in the work of Lippold and Lin [4]. For autogenous welding, the HCS is in general higher as for welding with an appropriate filler material. For non-autogenous welding, the choice of the filler material is also of great importance, as explicated in detail in the work of Kostrivas and Lippold [1] and Allen et al. [5]. Ellis [6] demonstrated that a high HCS generally results in a deterioration of the mechanical properties. Up to now, very few approaches for autogenous laser welding of aluminium alloys intending a reduction of the HCS have been developed. In most of the

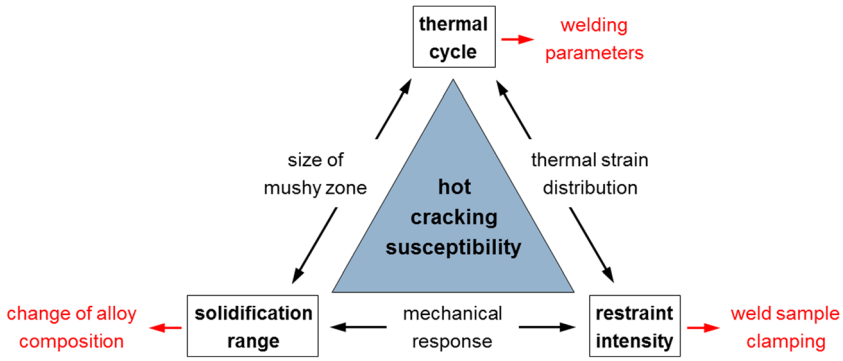

Fig. 1 Influencing factors on the hot cracking susceptibility according to Cross [8]

studies, only one specific aspect of HCS has been investigated.

The present study deals with the hot cracking susceptibility of the Al-Cu-Li alloy AA2198 during autogenous laser-beam welding. Three completely different approaches were applied to AA2198 with the objective of reduction or even prevention of hot cracking. The presented approaches were derived from the theoretical considerations of the causes for hot cracking known from the pertinent literature for other aluminium alloys and fusion-welding techniques. The effectiveness of the approaches was assessed by the measurement of the total crack length (TCL). Moreover, the mechanical properties autogenously laser welded samples were determined and compared to that of samples laser welded with an Al-Si filler wire. However, the use of filler wire is in certain cases not desired or even not possible, as for example for cost saving purposes or in case of structures with limited accessibility for welding, as for example described by Ion [7]. By comparing different approaches for reducing the HCS applied to the same material, it was possible to identify the most effective approach for a specific aluminium alloy, namely AA2198.

2 Factors affecting hot cracking susceptibility

Referring to the work of Cross [8], hot cracking occurs during the solidification of weld metal owing to the rupture of liquid films in the tailing mushy zone. During solidification of the melt pool, a remaining melt is situated at the crystallisation front, which is characterised by a lower solidification temperature compared with the ambient dendrites due to segregation. The formation of solidification cracks generally takes place towards the end of solidification process in weld pool, when the segregated residual melt included between the dendrites does not transmit shrinkage forces. In Fig. 1, the three main influencing factors on HCS of materials during fusion welding are specified.

The thermal cycle, resulting from the parameters used for welding, has an effect on the size of the mushy zone, in which hot cracking occurs. It is assumed that an enlarged mushy zone experiences more strain due to shrinkage, as described in the work of Cross [8]. The amount of strain in a liquid film is given by the solidification range resulting from the chemical composition and the cooling rate of the weld metal. Referring to the work of Kostrivas and Lippold [9], the HCS of aluminium alloys is maximum for 3.0 wt.% Cu, 3.0 wt.% Mg, 2.5 wt.% Li, and 0.8 wt.% Si, which is close to the chemical composition of many commonly used aluminium alloys. The change of chemical composition of the used material is often not intended, mainly because of the adjusted mechanical properties. However, due to vaporisation during deep penetration laser welding, a loss of volatile alloying elements (such as Li and Mg) can be observed, which is in general relatively small. In the case of the Al-Cu-Li alloy

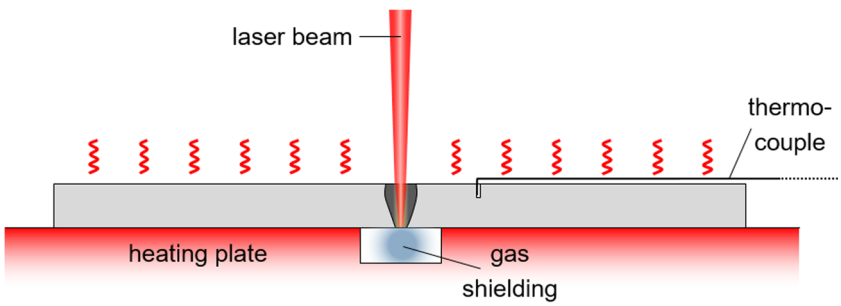

Fig. 2 Configuration for laser-beam welding with pre-heating

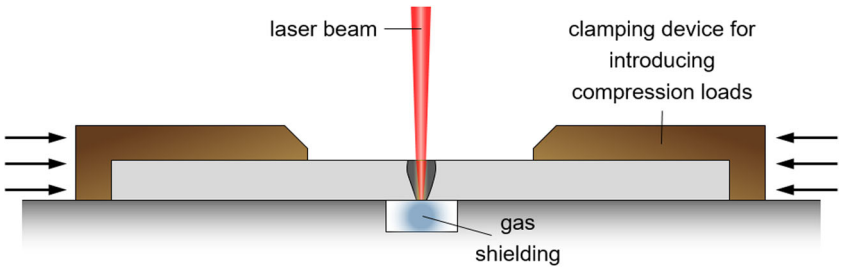

Fig. 3 Configuration for laser-beam welding with pre-loading

AA2198, the initial Li and Mg content is far below the critical amount for maximum HCS so that a potential loss of these volatile alloying elements would not have a detrimental effect on the hot cracking behaviour. Only by the addition of an appropriate filler material for laser welding, the solidification range of the weld metal can be locally adjusted. Referring to Katgerman and Eskin [10] and Dittrich et al. [11] for the fusion welding of Al-Cu alloys, the use of a filler wire with a high Si content (above the critical value of 0.8 wt.% for maximum HCS), such as AA4047 with 12 wt.% Si, is recommended, since the sufficient amount of liquid with eutectic composition facilitates the healing of the cracks. It was shown by Tian et al. [12] that solidification range of the Al-Cu-Li alloy AA2198 lies approximately between 500 and 650 °C, whereas AA4047 has a narrower solidification range (505 to 580 °C). According to Rappaz et al. [13], the most critical temperature range for HCS is assumed to lie at the end of the solidification with a solid fraction of 0.8 to 1. Alternatively, a filler wire containing grain refiners can also be used to reduce the HCS, as demonstrated by Mousavi et al. [14]. The extent of restraint strongly depends on the used clamping of the weld sample. It was also stated by Cross [8] that the interaction of the restraining forces and the local weld strains affect the strain and strain rate in the vicinity of the mushy zone.

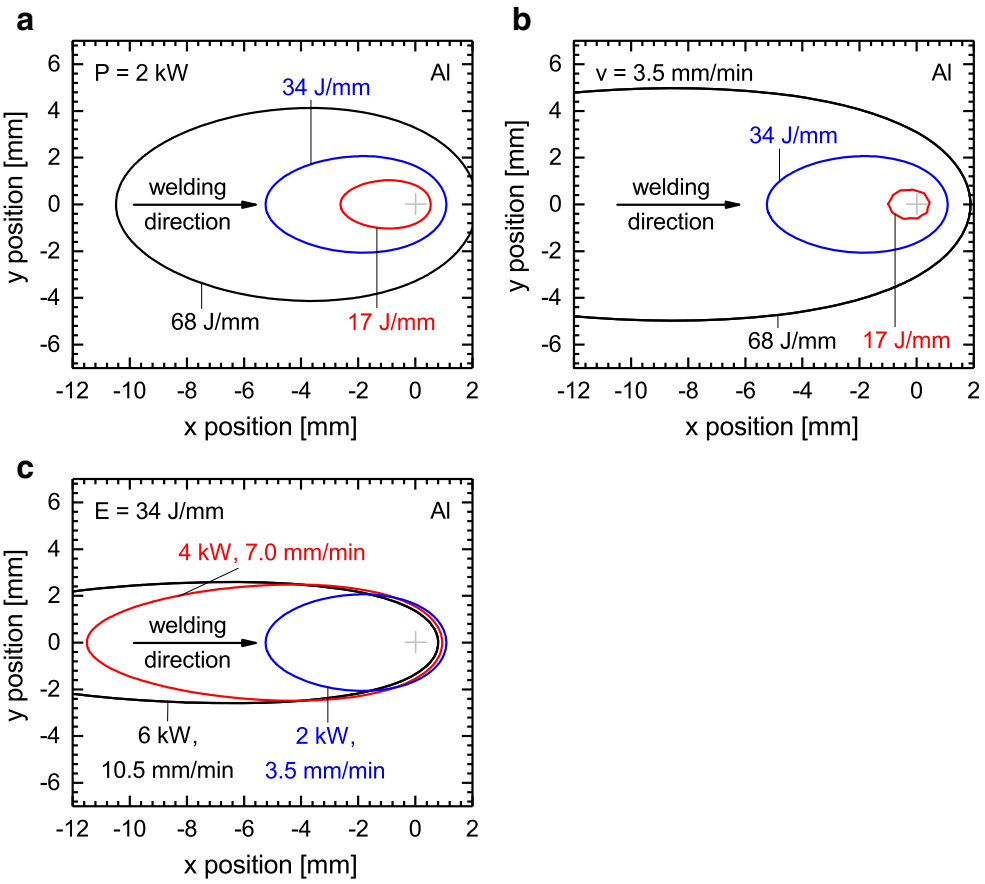

Fig. 4 Variation of melt pool size and shape for different welding velocities (**a**), different laser powers (**b**), and different combinations of laser power and welding velocity (**c**) (calculated with the help of the moving line source model described by Beyer [19] and in the work of Enz et al. [20])

Table 1 Chemical composition (in wt.-%) of the used aluminium alloys

Alloy	Cu	Li	Mg	Ag	Mn	Zn	Zr	Si	Fe	Ti	Al
AA2198	3.35	0.99	0.32	0.27	0.01	0.01	0.14	0.03	0.05	0.30	Bal.
AA4047	0.3	–	0.1	–	0.15	0.2	–	12.0	0.8	–	Bal.

3 Approaches for reducing the hot cracking susceptibility

3.1 Pre-heating of the weld samples

The first approach intends pre-heating of the weld samples to elevated temperatures during laser-beam welding in order to reduce the cooling rate. Thus, the thermal gradient in the weld sample shall be decreased, which finally results in a more even thermal contraction. Moreover, the time for strain release shall be extended, as suggested by Huang et al. [15]. In the work of Zhu et al. [16], the positive effect of pre-heating, in particular for pre-heating temperature of 200 °C and higher, on reducing the weld defects during conventional fusion welding of aluminium alloys was described. The pre-heating of the entire weld sample was performed using a large heating plate, on which the weld samples were placed. The temperature was monitored with the help of thermocouples on top of the weld sample. In order to avoid the oxide formation in the weld zone, shielding gas (Ar) was supplied from the root side, as depicted in Fig. 2. Due to thermal convection gas, shielding from the top side was counterproductive. For this study, the influence of three different pre-heating temperatures (120, 160, and 200 °C) on the HCS was investigated. The temperatures chosen for the pre-heating experiments lie in the temperature range used for artificial ageing of the precipitation-hardenable Al-Cu alloys, as described in the work of Wang et al. [17]. However, the heating times are relatively short in comparison to typical ageing treatments. Higher pre-heating temperature would lead to unintentional change of the microstructure and thus to a degradation of the mechanical properties.

3.2 Pre-loading of the weld samples

The second approach intends pre-loading of the weld samples during laser-beam welding. By introducing a compression load perpendicular to the welding direction, the effect of strain localization due to solidification shrinkage in the mushy zone shall be reduced or even compensated, since the liquid films at the grain boundaries are prone to tensile strains, as described in the work of Coniglio [18]. The pre-loading was performed using a tailored clamping device, as depicted in Fig. 3. In order to obtain reproducible compression force, a specific torque was adjusted with the help of a torque wrench. For this study, only one compression load level was tested.

3.3 Adjustment of the laser-welding parameters

The third approach intends the adjustment of the laser-welding parameters in order to influence the size of the mushy zone. A multitude of parameters can be used for this purpose. The enlargement of the laser focus spot diameter directly results in the increase of the melt pool and thus also of the trailing mushy zone. Moreover, the beam intensity is slightly lower for the larger focus spot diameter, when welding with the same laser-welding parameters. The beam intensity is the ratio of the laser power and the focus spot diameter. In this way, the thermal gradient in the weld zone is also reduced. The adjustment of the laser focus spot diameter can be done by the choice of the feeding fibre and the optical setup or by defocussing of the laser beam. Furthermore, the size and shape of the melt pool can also be adjusted by the choice of laser power and welding velocity. The ratio of laser power and welding velocity gives an estimation of the heat input and is also referred as line energy. By comparing Fig. 4a, b, it becomes obvious that influence of laser power is considerably higher as for the welding velocity. An increase of the laser power leads not only to a widening but also to a distinct elongation of the melt pool in welding direction. For similar heat inputs, realised with different combinations of laser power and welding velocity, differing melt pool sizes and shapes can result, as depicted in Fig. 4c. In this context, in particular, the

Table 2 Properties of the laser beam using different fibre diameters

Fibre diameter (μm)	Focal length (mm)	Collimator length (mm)	Focus spot diameter (μm)	BPP (mm mrad)
200	300	120	512	7.5
300			746	11.4

Table 3 Parameters for autogenous laser-beam welding with different heat inputs

No.	Laser power (kW)	Welding velocity (m/min)	Heat input (J/mm)
1	4	5.0	48
2	6	7.5	
3	8	10.0	
4	4	6.0	40
5	8	12.0	
6	4	7.0	34
7	6	10.5	
8	8	14.0	
9	4	8.0	30
10	6	12.0	

Table 4 Parameter for non-autogenous laser-beam welding

Laser power (kW)	Welding velocity (m/min)	Heat input (J/mm)	Wire feed rate (m/min)
3	2.2	82	1.3

length of the melt pool increases for large values of the welding velocity. By realising the same heat input with a lower laser power, smaller melt pools can be obtained. High heat inputs generally result in low thermal gradients and thus in a more even thermal contraction, as described earlier. Moreover, the amount of shielding gas (gas flow rate) used during laser-beam welding can have an influence on the cooling rate of the melt and thus also on the thermal gradient.

For the present study, two different feeding fibres (200 and 300 μm), four different heat inputs (30, 34, 40, and 48 J/mm) accomplished with different laser power, and welding velocity levels as well as two shielding gas conditions were used.

4 Materials and experimental methods

4.1 Materials

For the laser-beam welding experiments, the Al-Cu-Li alloy AA2198 with a T3 tempering was utilised. The chemical composition of this alloy is given in Table 1. The under-aged tempering condition of the precipitation-hardenable alloy was chosen in order to enable the application of an appropriate post-weld heat treatment and to avoid unintentional over-ageing due to pre-heating.

For autogenous laser welding, no additional filler wire was used. However, for comparison purposes, laser-beam welding with a filler wire was conducted. Therefore, the Al-Si alloy AA4047 was used (Table 1).

The sheets had a thickness of 3.2 mm. All laser welding experiments were conducted perpendicular to the rolling direction of the sheets.

4.2 Laser-beam welding

The laser-beam welding was performed using an Yb fibre laser (IPG YLS 8000) with a maximum laser power of 8.0 kW. For the first and the second approach, a fibre diameter of 200 μm was utilised. For the third approach, a second fibre diameter were used, which resulted in different laser focus spot diameters using the same optical device with a focal length of 300 mm and a collimator length of 120 mm. The resulting laser beam properties for both fibre diameters are summarised in Table 2. The focus spot diameter was measured with a laser beam diagnostic system (Primes Focus Monitor). The increase of the laser focus spot diameter by + 234 μm results in a reduction of the theoretical beam intensity of 53% for the same laser power.

Moreover, different laser parameters were used, which resulted in different heat inputs, as given in Table 3. All of the laser-welding parameters were chosen so that a full

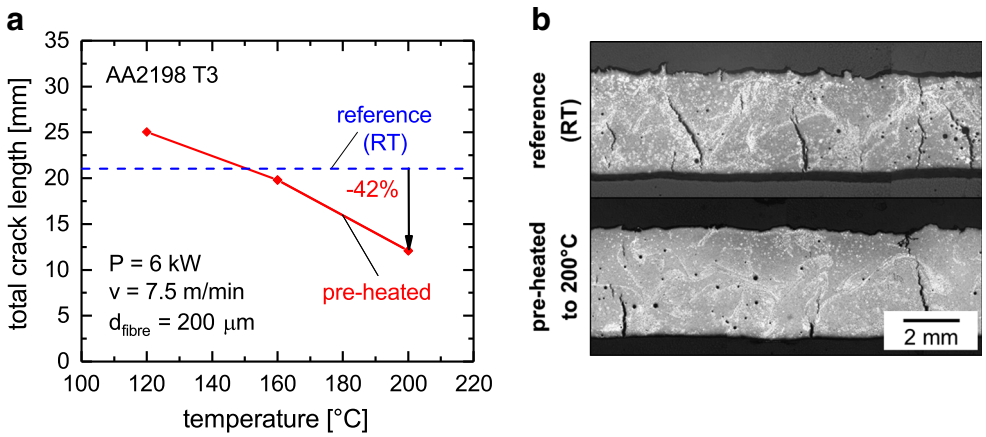

Fig. 5 Effect of the pre-heating temperature on the total crack length of AA2198 (**a**) and longitudinal section of a specimen laser welded (with one parameter set) at room temperature and pre-heated to 200 °C (**b**)

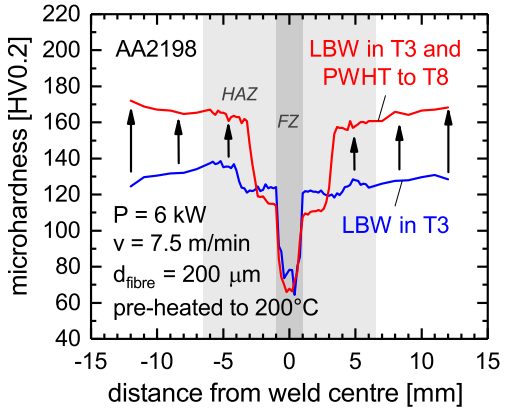

Fig. 6 Influence of the pre-heating on the microhardness of laser welded AA2198

penetration of the sheet was achieved. The welding velocity was realised by moving the laser optical system above the specimen with the help of a high-accuracy 6-axis industrial robot (KUKA KR 30HA).

For all autogenous welding experiments, argon was used as shielding gas, which was supplied only from the root side with a gas flow rate of 5 l/min. In order to enable the comparability with the first approach, for which no top gas shielding was possible, this one-sided gas shielding strategy was chosen for all approaches.

For comparison purposes, non-autogenous laser welding was also conducted. Therefore, the same laser fibre diameter and laser optical setup was used as for the first and second approach. The used parameters were determined in a preliminary study (Table 4). Due to the addition of a filler material, a higher heat input was required for achieving full penetration. Helium was used as shielding gas, which was supplied from top and root side with a flow rate of 30 l/min.

4.3 Assessment of the weld quality

For assessing the quality of the obtained welds with special regard to the HCS, macrographs of longitudinal-sectioned specimens were taken. Therefore, the samples were cut, grinded, and polished as target preparation for the centre of the fusion zone. In addition, macrographs of cross-sections were also taken. All sections were etched using Dix-Keller reagent in order to achieve the visibility of the microstructure. The TCL, defined as the sum of all cracks along the entire weld seam, were determined using an image processing software for the longitudinal sections. Non-destructive testing, such as radiographic or penetration testing, does either have a limited resolution for detecting low-volume cracks or can solely detect surface cracks and was therefore not applied for the quantification of the HCS.

The local mechanical properties, in terms of microhardness profiles, were determined (according to DIN EN ISO 6507-1) using a semi-automated Vickers microhardness testing machine (Shimadzu HMV-2000) with a test load of 1.961 N and an indentation time of 20 s was used. Flat tensile specimens were used to investigate the global mechanical properties under tensile load (according to DIN ISO 6892-1) with flat tensile specimens. For this purpose, an electro-mechanical testing machine with 100 kN load cell (SchenkTrebel RM100) was used. A constant testing speed of 0.5 mm/min was applied for tensile testing. The elongation was measured contact free with the help of a laser extensometer (Fiedler WS-160).

5 Results and discussion

Using the recommended AA4047 filler wire with high Si content in a sufficient quantity for welding, Al-Cu-Li resulted in crack free weld. In the longitudinal section no cracks were detected.

5.1 Effect of pre-heating

In comparison to the reference weld, laser welded autogenously with the same welding parameters but without pre-heating, a considerable reduction of the TCL was only achieved for pre-

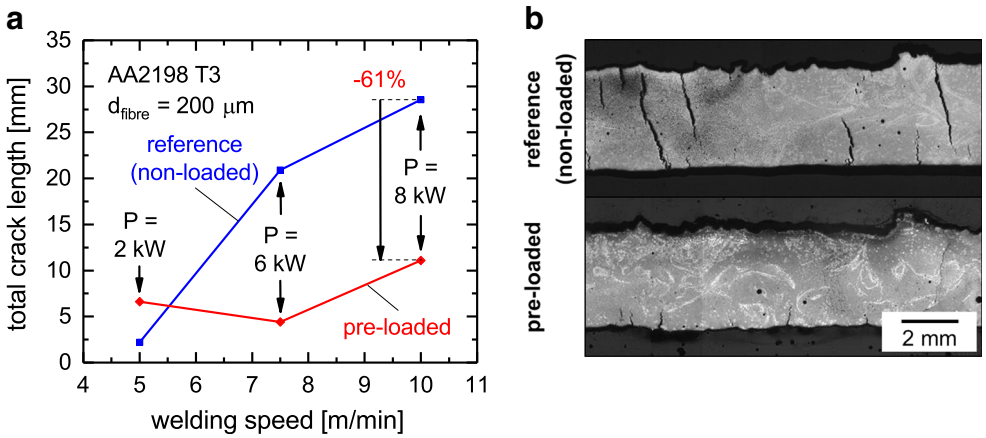

Fig. 7 Influence of the pre-loading on the total crack length of AA2198 laser welded with three different parameter sets but with a constant heat input of 48 J/mm (**a**) and longitudinal section of a non-loaded and pre-loaded specimen laser welded with a laser power of 8 kW (**b**)

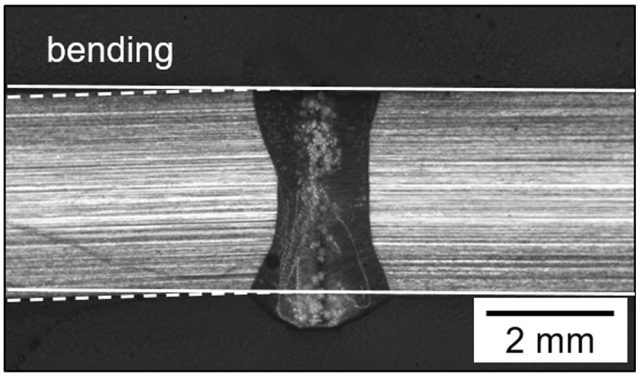

Fig. 8 Cross-section of a specimen laser welded with preloading showing slight bending

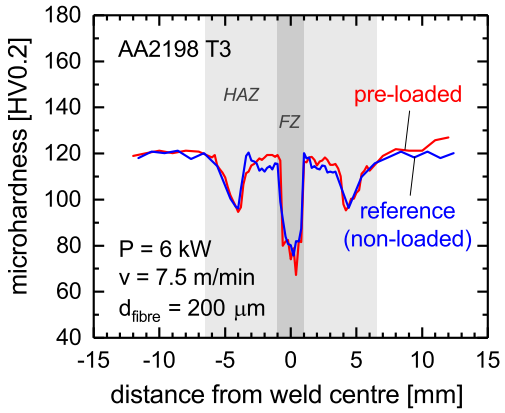

Fig. 9 Effect of pre-loading on the microhardness of laser welded AA2198

heating temperatures higher than160 °C, as it can be seen in Fig. 5a. For the pre-heating temperature of 200 °C, a TCL reduction of up to 42% was achieved, when compared to the reference weld laser welded at room temperature (RT). The welds showed almost no reduction of the frequency of the occurrence of cracks, but considerable shorter cracks (Fig. 5b). And the majority of the cracks seem to nucleate from the weld seam surface and propagating to the centre of the weld seam. However, for the pre-heating temperature of 120 °C, the hot cracking seemed to be slightly aggravated above the level of the reference weld laser weld at room temperature.

The occurrence of the same amount of cracks with shorter lengths implies that the crack propagation was inhibited but not the crack nucleation. The amount of crack nucleation sites, such as pores or inclusions, could not solely be reduced by pre-heating. Due to the fact that the chemical composition of the alloy was kept constant, the solidification range and thus the maximum amount of liquid film could not be changed. However, by pre-heating, it is possible to reduce the cooling rate. In this way, the time for solidification is prolonged. Moreover, the rupture of the liquid film, as a mechanism for crack propagation during solidification described by Katgerman and Eskin [10], was inhibited to certain extend by the more even thermal contraction and the extended time for strain release.

The contradictory hot cracking behaviour observed for a pre-heating temperature of 120 °C cannot be explained with the currently known theory for HCS. It is assumed that an unknown external factor could have caused the slightly increased TCL, whereas the influence of statistical scattering is assumed to be small. From the theoretical considerations, a value close to the TCL of the reference welded at room temperature is expected.

The welded sample pre-heated to 200 °C showed in the heat-affected zone as well as in the base material an approximately 10 HV0.2 higher microhardness than the reference sample, laser welded at room temperature, as it can be seen in Fig. 6. Moreover, no severe hardness degradation in the heat-affected zone occurs as for the reference sample. However, no improvement of the hardness was achieved for the fusion zone.

The decrease of hardness in the heat-affected zone by the dissolution of the metastable precipitates. The reason for the improved microhardness in the heat-affected zone and the base material of the pre-heated sample lies in the initial tempering condition T3 condition, which enables to some extend

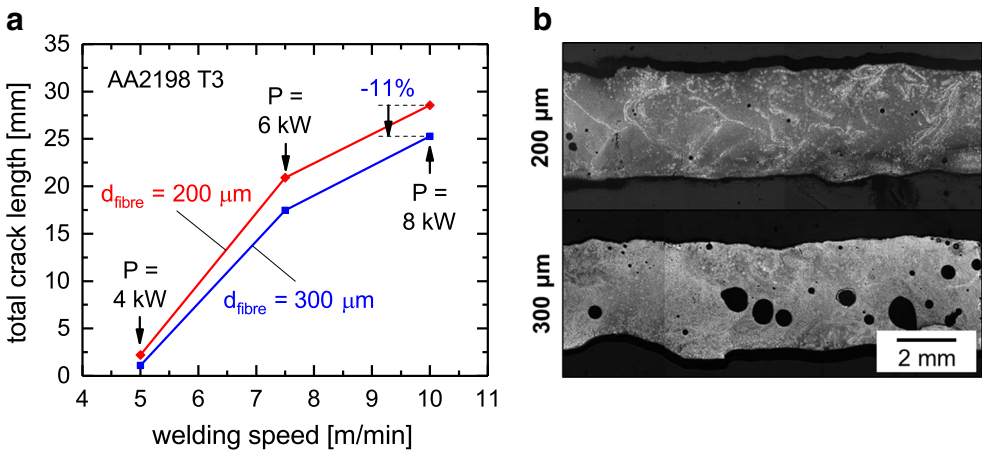

Fig. 10 Influence of the laser focus spot diameter on the total crack length of AA2198 (**a**) and longitudinal section of a specimen laser welded with a 200- and 300-µm fibre and a laser power of 6 kW (**b**)

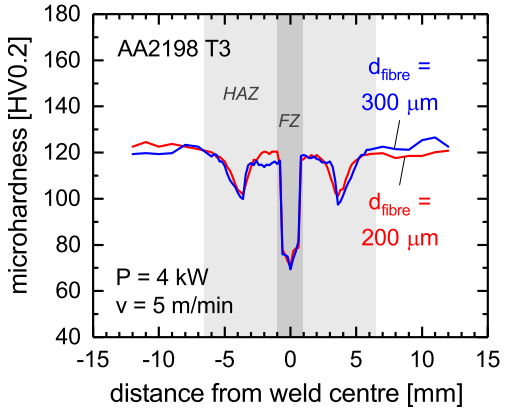

Fig. 11 Effect of the laser focus spot diameter on the microhardness of laser welded AA2198

ageing during the pre-heating treatment. The influence of different heating temperatures between 170 and 210 °C on an under-aged AA2198 sheet was for example investigated by Alexopoulos et al. [21]. The distinct hardness drop in the fusion zone can be explained by the fact that due to melting and subsequent solidification, the microstructure was completely changed. As explained earlier, it is also possible that the chemical composition could be slightly changed due to the vaporisation of volatile alloying elements during deep penetration laser welding. The temper condition after laser welding corresponds to the as-fabricated condition, since no special control of the heating and cooling has been performed during welding.

5.2 Effect of pre-loading

Pre-loaded samples for laser welding generally showed low level of TCL. However, for low laser power and welding velocity levels, the TCL was slightly above the level of the reference sample, laser welded with the same parameters, as shown in Fig. 7a. Again, the pre-loaded samples, laser welded with higher laser power and welding velocity, exhibited considerable shorter crack lengths, which predominantly nucleated from the surface (Fig. 7b). For a laser power of 8 kW, a reduction of the TCL of approximately 61% was possible in comparison to the reference welds.

The reason for the reduced crack propagation during solidification lies again in the inhibition of the liquid film rupture. The applied compression load support the transmission of shrinkage forces from the residual melt to the ambient solidified microstructure and thus counteracts to some extend the shrinkage strains in the welding zone. Due to the fact that the welding zone was very localised running through the sheet, and the compression load was always applied to the entire sample, it is assumed that the stress and strain condition might differ along the weld line. This could limit the reproducibility of the results and also the transferability to more complex structures.

Furthermore, a slight, but unintended, bending of the sample was observed due to the pre-loading perpendicular to the welding direction, as it can be seen in Fig. 8.

The microhardness profiles of the pre-loaded and the reference sample do not differ from the reference welds (Fig. 9), since the same parameters were used for laser welding. This means that both samples experience the same thermal history.

5.3 Effect of the laser focus spot diameter

The influence of the used fibre diameter and thus of the resulting focus spot diameter on the TCL is comparatively very limited. In Fig. 10a, it can be seen that an increase of the focus spot diameter from 512 µm for the 200-µm fibre to 746 µm for the 300 µm led only to a reduction of the TCL of approximately 11% for a laser power of 8 kW resulting in a high HCS. Surprisingly, the sample laser welded with the larger focus spot diameter exhibit comparatively high porosity.

The slight improvement of the HCS for the larger focus spot diameter can be mainly explained by the increase of the melt pool width. The size of the trailing mushy zone is not

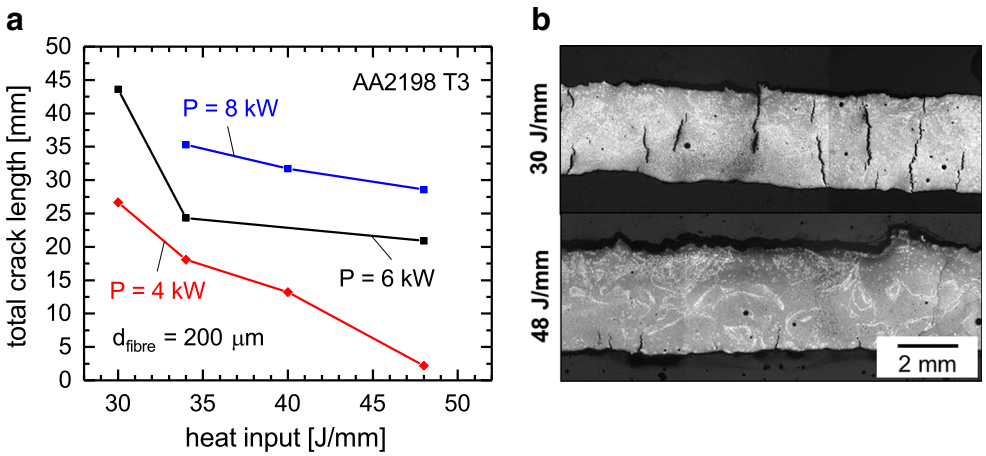

Fig. 12 Influence of the heat input on the total crack length of AA2198 (**a**) and longitudinal section of a specimen laser welded with a heat input of 30 and 48 J/mm and a laser power of 6 kW (**b**)

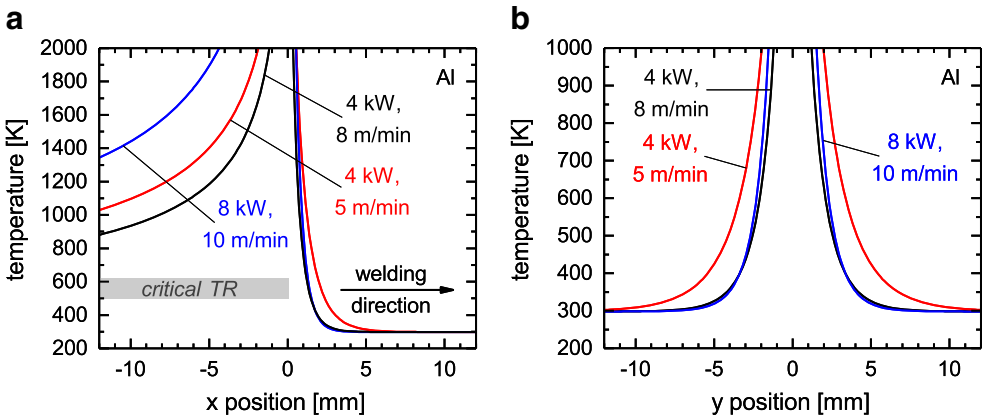

Fig. 13 Calculated temperature distribution for three different welding parameters (calculated based on the moving line source model described by Beyer [19] and in the work of the authors [20])

expected to increase considerably, due to the fact that the beam intensity is smaller for the larger focus spot diameter. Moreover, this can also result in a slightly lower thermal gradient in the welding zone. The presence of large pores in the fusion zone of the weld indicates the occurrence of keyhole instabilities during welding with the larger focus spot diameter for the given welding parameters.

The microhardness profiles of the sample laser welded with the same laser power and welding velocity, but different focus spot diameters resemble each other in appearance (Fig. 11). Although a lower beam intensity results for the larger focus spot diameter, no influence on the microstructure and thus on the microhardness was determined.

5.4 Effect of the laser power, welding velocity, and heat input

The largest effects on the TCL were observed for the variation of the laser power and the welding velocity, as it is shown in Fig. 12a. It turned out that low laser power levels and low welding velocities resulted in the small TCL's. The lowest TCL (with 2.2 mm) was achieved for 4 kW and 5 m/min yielding in a high heat input of 48 J/mm (later referred as optimised autogenous laser welding parameters). The frequency of occurrence as well as the length of the single cracks could be reduced with this approach, as it can be seen in Fig. 12b. However, for similar heat inputs implemented with different welding parameters, the crack lengths can differ considerably.

As mentioned above, the size and shape of the melt pool strongly depend on the laser power and the welding velocity (Fig. 4a, b). And even for similar heat inputs, different melt pool sizes can result (Fig. 4c). From this theoretical considerations and the experimental results, it can be assumed that a small melt pool and in particular a small trailing mushy zone has a beneficial effect on the HCS of AA2198 even in case of high heat inputs. This is contrary to the study of Cross [8], in which it was stated that high inputs generally result in larger TCL.

In addition, the consideration of the temperature profile for the different welding parameter sets (Fig. 13) showed that the thermal gradient for the optimised welding parameters (4 kW and 5 m/min) lies in welding direction (x direction) between profiles for the welding parameters, which both resulted in considerable higher TCL's. However, in y direction (perpendicular to the welding direction), the temperature profile for the optimised welding parameters differ from the other two profiles. The thermal gradient in the critical temperature range (TR) between 500 °C (773 K) and 610 °C (883 K) during solidification (referring to Tian et al. [12]) is noticeable lower

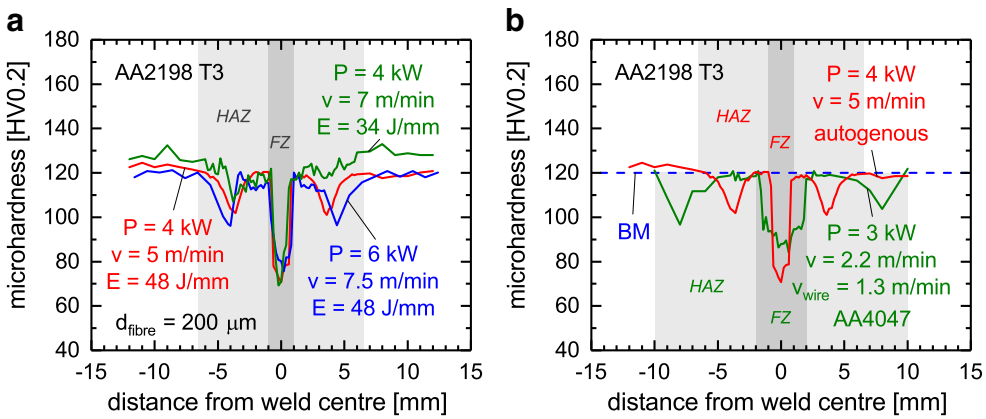

Fig. 14 Influence of the welding parameters (**a**) and the use of AA4047 filler wire (with adjusted laser-welding parameters) (**b**) on the microhardness

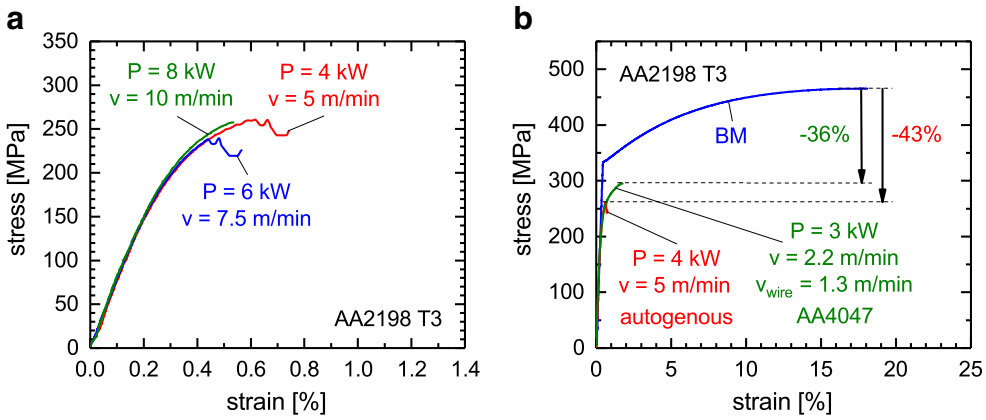

Fig. 15 Influence of the heat input (**a**) and the use of AA4047 filler wire (with optimised laser-welding parameters) (**b**) on the tensile properties

as for the other welding parameters. For this reason, the sample welded with 4 kW and 5 m/min showed a lower TCL, although the melt pool is larger as for the sample welded with the same laser power but 8 m/min. This means that besides the size of the trailing mushy zone, the low thermal gradients are of great importance in order to improve the HCS of AA2198. The obtained results correspond to the findings of earlier studies of Wang et al. [22] and Tian et al. [12].

The microhardness profiles in Fig. 14a show also differences caused by the dissimilar heat inputs and melt pool dimensions. For high welding velocities, the hardness degradation in the heat-affected zone is lower as for the samples with the same laser power but lower welding velocities. Even for the same heat input, different hardness profiles are obtained. Here, higher laser power levels result in a larger hardness drop in the heat-affected zone. By comparing the optimised autogenous laser, welding parameter with the optimised parameters for laser welding with AA4047 filler wire, it can be seen that the fusion zone and the heat-affected zone of the autogenously welded sample are considerable narrower. However, the hardness drop in the fusion zone is slightly higher.

The optimised welding parameters also resulted in slightly improved tensile properties in terms of tensile strength and strain to failure, when compared to the other autogenous welds (Fig. 15). The tensile strength of the sample laser welded with filler wire is only 7% higher as the optimised autogenously welded sample, when compared to the base material. The ductility of both sample laser welded with filler wire and laser welded autogenously is comparable low with 1.8 and 0.7% strain, respectively. However, this is typical for welded precipitation hardenable aluminium alloys.

A joint efficiency of 57% for the optimised autogenous welding parameters corresponds to the results obtained for other Al-Li alloys laser welded autogenously (with joint efficiencies of 53–59.8%), as summarised in the work of Xiao et al. [22] and Ning et al. [23].

5.5 Effect of the shielding gas

Finally, it was demonstrated that also the amount of shielding gas has a certain influence on the HCS. In Fig. 16a, it can be seen that without the use of the top shielding gas and a lower gas flow rate at the root side, it was possible to reduce the TCL by approximately 82%. Surprisingly, the sample laser welded without top shielding gas exhibited a lower porosity level.

The explanation for this improvement of the HCS can be found in the cooling effect of the shielding gas, which results in higher thermal gradients on the top surface. In spite of the

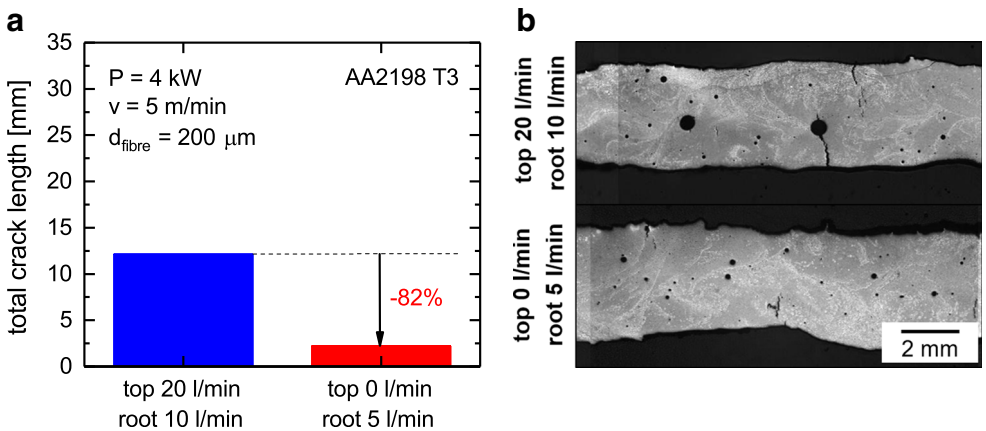

Fig. 16 Influence of the top shielding gas supply on the total crack length of AA2198 (**a**) and longitudinal section of a specimen laser welded with and without top shielding (**b**)

positive effect of laser welding without top shielding gas on the HCS, this approach is often not applicable for aluminium alloys due to the fact that the improper gas shielding generally result in rapid growth of the oxide layer on the surface and in the formation of porosity. It was shown by Enz et al. [24] that a large laser beam diameter can have a positive effect on the degassing behaviour of the melt pool during laser welding of aluminium alloys. This could be the explanation for the slightly lowered porosity level. Nevertheless, low gas flow rates and/or an improved shielding strategy are generally recommended, in order to provide complete shielding of the melt pool but also to avoid unintended too fast cooling of the melt. Only in this way, welds with a high weld quality, in matters of low porosity and low hot cracking, can be obtained.

6 Conclusions

Based on the results obtained from this study, the following conclusion can be drawn:

1. Each of the three approaches for improving the hot cracking susceptibility of autogenously laser beam welded Al-Cu-Li alloy AA2198 presented in this study, resulted in a reduction of the total crack length and thus to an improvement of the hot cracking sensitivity.
2. In direct comparison, the greatest improvement in terms of the lowest total crack length was achieved for the third approach intending a high heat input for laser welding realised with low laser power and low welding velocity, since these parameters result in small melt pool and low thermal gradients.
3. With regard to the resulting mechanical properties, the third approach for autogenous laser welding proposed in this study is competitive with non-autogenous laser welding intending the use an Al-Si filler wire.
4. The variety of available and effective approaches for improving the hot cracking susceptibility of aluminium alloys enables autogenous laser welding tailored to the specifications of the structure and the process conditions.

6.1 Remarks to the industrial applicability

Due to the promising results for optimised autogenous laser-welding parameters and the high industrial implementation potential of this approach, an abandonment of a filler wire for the laser welding of the Al-Cu-Li alloy AA2198 could already be justified. Although pre-heating and pre-loading also resulted in an improvement of the hot cracking susceptibility, the higher manufacturing effort and the limited transferability to complex structure could limit their industrial applicability. Moreover, an incorrect application of these two approaches could also lead to an aggravation of the hot cracking susceptibility. The abandonment of shielding gas is also often not applicable due to the possibility of increased porosity formation. However, improved gas shielding strategies with low gas flow rates should be considered for industrial application.

References

1. Kostrivas A, Lippold JC (1999) Weldability of Li-bearing aluminium alloys. Int Mater Rev 44:217–237. https://doi.org/10.1179/095066099101528289
2. Srivatsan TS, Sudarshan TS (1991) Welding of lightweight aluminium-lithium alloys. Weld J 70:173–184
3. Giummarra C, Thomas B, Rioja RJ (2007) New aluminum lithium alloys for aerospace applications. In: Proc Light Met Technol Conf 2007
4. Lippold JC, Lin W (1996) Weldability of commercial Al-Cu-Li alloys. Mater Sci Forum 217:1685–1690. https://doi.org/10.4028/www.scientific.net/MSF.217-222.1685
5. Allen CM, Verhaeghe G, Hilton PA, Heason CP, Prangnell PB (2006) Laser and hybrid laser-MIG welding of 6.35 and 12.7 mm thick aluminium aerospace alloy. Mater Sci Forum 519:1139–1144. https://doi.org/10.4028/www.scientific.net/MSF.519-521.1139
6. Ellis MBD (1996) Fusion welding of aluminium-lithium alloys. Weld Metal Fabr 64:55–60
7. Ion JC (2000) Laser beam welding of wrought aluminium alloys. Sci Techol Weld Join 5:265–276. https://doi.org/10.1179/136217100101538308
8. Cross CE (2005) On the origin of weld solidification cracking. In: Böllinghaus T, Herold H (eds) Hot cracking phenomena in welds I. Springer-Verlag, Berlin, pp 3–18. https://doi.org/10.1007/3-540-27460-X_1
9. Kostrivas A, Lippold JC (1999) Weldability of Li-bearing aluminium alloys. Int Mat Rev 44(6):217–237. https://doi.org/10.1179/095066099101528289
10. Katgerman L, Eskin DG (2005) In search of the prediction of hot cracking in aluminium alloys. In: Böllinghaus T, Herold H (eds) Hot cracking phenomena in welds II. Springer-Verlag, Berlin, pp 11–26. https://doi.org/10.1007/978-3-540-78628-3_1
11. Dittrich D, Standfuss J, Liebscher J, Brenner B, Beyer E (2011) Laser beam welding of hard to weld Al alloys for regional aircraft fuselage design—first results. Phys Proc 12:113–122. https://doi.org/10.1016/j.phpro.2011.03.015
12. Tian Y, Robson JD, Riekehr S, Kashaev N, Wang L, Lowe T, Karanika A (2016) Process optimization of dual-laser beam welding of advanced Al-Li alloys through hot cracking susceptibility modelling. Metall Mater Trans A 47:3533–3544. https://doi.org/10.1007/s11661-016-3509-4
13. Rappaz M, Drezet JM, Gremaud M (1999) A new hot-tearing criterion. Metall Mater Trans A 30:449–456. https://doi.org/10.1007/s11661-999-0334-z
14. Mousavi MG, Cross CE, Grong Ø (1999) Effect of scandium and titanium-boron on grain refinement and hot cracking of aluminium alloy 7108. Sci Technol Weld Join 4:381–388. https://doi.org/10.1179/136217199101538030
15. Huang H, Fu PH, Wang YX, Peng LM, Jiang HY (2014) Effect of pouring and mold temperatures on hot tearing susceptibility of AZ91D and Mg–3Nd–0.2 Zn–Zr Mg alloys. Trans Nonferrous Metals Soc China 24:922–929. https://doi.org/10.1016/S1003-6326(14)63144-7

16. Zhu C, Tang X, He Y, Lu F, Cui H (2018) Effect of preheating on the defects and microstructure in NG-GMA welding of 5083 Al-alloy. J Mat Process Technol 251:214–224. https://doi.org/10.1016/j.jmatprotec.2017.08.037
17. Wang CS, Starink MJ, Gao N (2006) Precipitation hardening in Al-Cu-Mg alloys revisited. Scr Mater 54:287–291. https://doi.org/10.1016/j.scriptamat.2005.09.010
18. Coniglio N (2008) Aluminium alloy weldability: identification of weld solidification cracking mechanisms through novel experimental technique and model development. Doctoral thesis; Otto von Guericke University Magdeburg
19. Beyer E (1995) Schweißen mit Laser: Grundlagen. Springer-Verlag, Berlin. https://doi.org/10.1007/978-3-642-75759-4
20. Enz J, Riekehr S, Ventzke V, Huber N, Kashaev N (2016) Laser weldability of high-strength Al-Zn alloys and its improvement by the use of an appropriate filler material. Metall Trans A 47:2830–2741. https://doi.org/10.1007/s11661-016-3446-2
21. Alexopoulos ND, Proiou A, Examilioti T, Kashaev N, Riekehr S, Kourkroulis SK (2016) Effect of artificial aging on the mechanical performance of (Al-Cu) 2024 and (Al-Cu-Li) 2198 aluminum alloys. Proc Struct Integr 2:3782–3783. https://doi.org/10.1016/j.prostr.2016.06.470
22. Wang X, Lu F, Wang HP, Qu Z, Xia L (2016) Micro-scale model based study of solidification cracking formation mechanism in Al fiber laser welds. Mat Process Technol 231:18–26. https://doi.org/10.1016/j.jmatprotec.2015.12.006
23. Ning J, Zhang LJ, Bai QL, Yin XQ, Niu J, Zhang JX (2016) Comparison of the microstructure and mechanical performance of 2A97 Al-Li alloy joints between autogenous and non-autogenous laser welding. Mat and Des 120:144–156. https://doi.org/10.1016/j.matdes.2017.02.003
24. Enz J, Riekehr S, Ventzke V, Huber N, Kashaev N (2016) Fibre laser welding of high-alloyed Al-Zn-Mg-Cu alloys. J Mat Process Technol 237:155–162. https://doi.org/10.1016/j.jmatprotec.2016.06.002